

Unified Embodied VLM Reasoning with Robotic Action via Autoregressive Discretized Pre-training

Yi Liu^{1*}, Sukai Wang^{1*†}, Dafeng Wei¹, Xiaowei Cai¹, Linqing Zhong¹, Jiange Yang¹, Guanghui Ren², Jinyu Zhang^{1,3}, Maoqing Yao², Chuankang Li¹, Xindong He¹, Liliang Chen¹, Jianlan Luo^{1,3‡}

¹AgiBot Research

²AgiBot

³Shanghai Innovation Institute

Abstract—General-purpose robotic systems operating in open-world environments must achieve both broad generalization and high-precision action execution, a combination that remains challenging for existing Vision-Language-Action (VLA) models. While large Vision-Language Models (VLMs) improve semantic generalization, insufficient embodied reasoning leads to brittle behavior, and conversely, strong reasoning alone is inadequate without precise control. To provide a decoupled and quantitative assessment of this bottleneck, we introduce Embodied Reasoning Intelligence Quotient (ERIQ), a large-scale embodied reasoning benchmark in robotic manipulation, comprising 6K+ question-answer pairs across four reasoning dimensions. By decoupling reasoning from execution, ERIQ enables systematic evaluation and reveals a strong positive correlation between embodied reasoning capability and end-to-end VLA generalization. To bridge the gap from reasoning to precise execution, we propose FACT, a flow-matching-based action tokenizer that converts continuous control into discrete sequences while preserving high-fidelity trajectory reconstruction. The resulting GenieReasoner jointly optimizes reasoning and action in a unified space, outperforming both continuous-action and prior discrete-action baselines in real-world tasks. Together, ERIQ and FACT provide a principled framework for diagnosing and overcoming the reasoning-precision trade-off, advancing robust, general-purpose robotic manipulation. Project page: <https://geniereasoner.github.io/GenieReasoner/>

I. INTRODUCTION

The pursuit of general-purpose robotic systems capable of operating autonomously in unstructured, open-world environments represents a fundamental challenge in artificial intelligence [1], [2], [3], [4], [5]. This endeavor necessitates simultaneous achievement of two critical, yet often competing objectives: achieving *broad generalization* across diverse, unseen scenarios [6], [7] while maintaining *high-precision action execution* for reliable task completion [8], [9], [10]. Recent advances in Large Vision-Language Models (VLMs), pre-trained on extensive internet-scale datasets, have established a new research direction by enabling the integration of rich

semantic knowledge derived from diverse multimodal data, thereby significantly enhancing generalization capabilities for downstream tasks. These advances have led to Vision-Language-Action (VLA) models that extend VLMs’ reasoning capability to directly predict robotic actions, unifying perception, reasoning, and control, establishing a principled bridge between abstract semantic reasoning and concrete low-level physical execution [4], [6], [5], [11], [3], [12], [1], [2], [13], [7], [14], [15], [16], [17], [18].

We posit that robust *embodied reasoning* is an indispensable prerequisite for achieving broad generalization in unstructured, dynamically evolving environments. This capability encompasses the synthesis of spatial awareness, temporal dynamics, and causal logic to explicitly plan, monitor, and adaptively correct physical actions. Without sufficient reasoning capabilities, learned policies are prone to falling back on superficial shortcuts derived from visual-action correlations, leading to brittle performance under distribution shifts, novel object configurations, or unexpected environmental perturbations [19], [11], [20]. However, possessing strong embodied reasoning capabilities, while necessary, is fundamentally insufficient in isolation; achieving reliable task completion in real-world scenarios equally demands *high-precision action execution*—the ability to generate exact, fine-grained control signals that faithfully translate abstract reasoning into precise physical movements. While VLA models in principle offer a unified framework capable of both precise robotic control and advanced reasoning, empirical observations suggest a persistent tension: models optimized for strong reasoning capabilities tend to exhibit reduced action precision, while those achieving high-fidelity execution often demonstrate limited generalization [20], [12]. This limitation hinders current VLA systems from achieving robust, real-world performance where both capabilities are essential [6].

To address these issues and provide a principled diagnostic framework, we introduce the Embodied Reason-

*Equal contribution †Project leader ‡Corresponding author

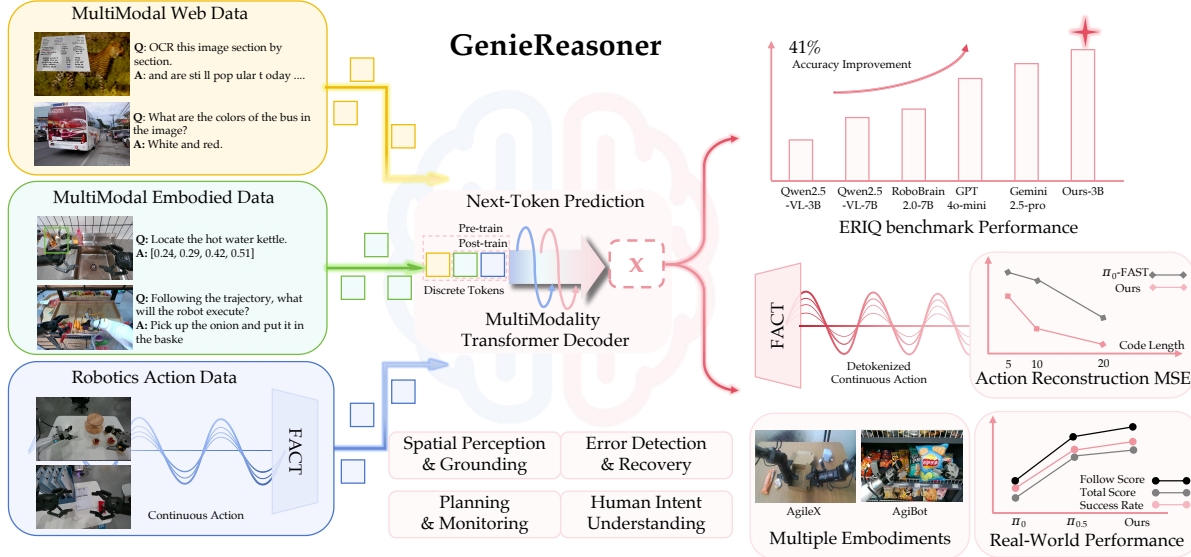


Fig. 1: We introduce the GenieReasoner system. (Left) Our system leverages large-scale general and embodied multimodal data to co-optimize high-level reasoning and low-level control within a unified autoregressive transformer. (Center) To bridge the gap between discrete planning and continuous execution, we introduce FACT, a novel action tokenizer that utilizes flow matching to reconstruct high-fidelity trajectories from quantized tokens. (Right) This unified design yields state-of-the-art results: GenieReasoner achieves a 41% accuracy improvement on our proposed ERIQ for embodied reasoning and demonstrates significantly lower reconstruction error (MSE) compared to π_0 -FAST. Consequently, our model outperforms flow-based baselines (e.g., $\pi_{0.5}$) in real-world robot manipulation tasks.

ing Intelligence Quotient (ERIQ), a large-scale benchmark for embodied reasoning in robotic manipulation. ERIQ decouples cognitive reasoning from motor control, enabling independent quantification of embodied reasoning without confounding action execution errors. ERIQ comprises 6K+ embodied question-answer pairs across four key reasoning dimensions. This scale enables comprehensive evaluation of reasoning capabilities, and provides a rich source of diverse reasoning scenarios for systematic analysis of the reasoning-generalization relationship. Empirical analysis on ERIQ reveals a strong positive correlation between VLM reasoning capabilities and end-to-end VLA generalization performance (detailed in Section V), suggesting that reasoning capabilities significantly influence generalization.

Achieving high-precision action execution requires bridging discrete semantic representations from language-centric reasoning tokens with continuous control signals for physical execution. One class of methods discretizes continuous robotic actions to enable co-training with VLM tokens. This approach faces a precision-efficiency trade-off: simple uniform binning necessitates an prohibitive number of tokens to achieve fine-grained control, consuming valuable context space [2], [3]; learned quantization (e.g., VQ-VAE [21], [22]) offers compact codes but lacks

high-precision control, often failing to reproduce the exact continuous signals required for dexterity; and rule-based adaptive schemes (e.g., FAST [12]) rely on variable-length encodings, where the non-deterministic structure frequently leads to decoding failures [23]. Hybrid architectures (e.g., π_0 [4]) append continuous prediction heads to discrete VLM backbones. However, joint training with conflicting objectives—discrete cross-entropy for tokens versus continuous regression for actions—can degrade reasoning performance [20].

To tackle this problem, we present FACT (Flow-matching Action Tokenizer), a discrete action tokenizer that leverages flow-matching to reconstruct high-fidelity continuous trajectories from compact token sequences. FACT transforms motor control into a discrete sequence modeling while preserving continuous-space precision. This enables the GenieReasoner (illustrated in Figure 1) to co-optimize reasoning and action within a unified gradient space. This alignment directly projects the VLM’s reasoning capabilities into precise actions, avoiding the generalization penalty of continuous heads while surpassing the fidelity limits of existing discrete tokenizers. Empirical evaluation demonstrates that GenieReasoner achieves superior performance over both continuous-action baselines (e.g., $\pi_{0.5}$ [6]) and discrete-action baselines (e.g., π_0 -FAST [12]), effectively balancing em-

bodied reasoning and action precision across diverse benchmarks and real-world robotic deployments.

Our key contributions are twofold. First, we introduce ERIQ, a large-scale embodied reasoning benchmark, comprising over 6K question-answer pairs across four critical reasoning dimensions. Through systematic evaluation on ERIQ, we establish a strong positive correlation between embodied reasoning capabilities and generalization performance, providing empirical evidence that robust reasoning is essential for achieving broad generalization in open-world scenarios. Second, we present FACT, a flow-matching-based action tokenizer that reconciles the reasoning-precision trade-off by discretizing continuous action control into discrete sequence modeling while preserving high-fidelity trajectory reconstruction. The resulting GenieReasoner achieves state-of-the-art performance through unified co-optimization of embodied reasoning and precise action execution within a single gradient space.

Our results suggest that embodied reasoning is a key ingredient for enabling long-horizon, precise manipulation behaviors. We envision ERIQ serving as a valuable diagnostic tool for systematically evaluating and improving reasoning capabilities in future VLA models, and that FACT’s flow-matching approach will inspire new directions in bridging discrete semantic representations with continuous control for more capable robotic systems.

II. RELATED WORKS

The development of GenieReasoner is situated at the intersection of abstract semantic reasoning and high-precision physical control. To contextualize our contributions, we survey the literature across two primary dimensions: embodied reasoning frameworks and the evolution of VLA architectures.

A. Embodied Reasoning and Benchmarks

As robotic systems scale beyond primitive execution, research has focused on the intersection of high-level reasoning and low-level control, necessitating robust benchmarks to evaluate these embodied reasoning capabilities.

a) Hierarchical Planning: Early research in hierarchical planning utilized pre-trained or fine-tuned Large Language Models (LLMs) to decompose complex goals into high-level sub-tasks, which were then executed by specialized low-level policies [24], [25], [26], [27], [28], [29], [30], [31], [32], [33]. Subsequent efforts have focused on developing more structured reasoning systems. For instance, industrial-scale projects such as Genimi Robotics [7] augment sub-task planning with auxiliary information—including affordance estimation and detection results—to better guide low-level control.

Similarly, frameworks like RoboBrain [34] aim to endow VLMs with specific embodied capabilities, such as planning and affordance perception, through fine-tuning the model on curated, fine-grained datasets. However, such separation between high-level reasoning and low-level action prediction often results in misalignment, where the physical agent fails to adhere strictly to the reasoning instructions.

b) Reasoning Integration and Co-training: To bridge the gap between abstract planning and physical execution, recent frameworks integrate reasoning directly into the policy’s inference pipeline, either through explicit intermediate traces or implicit large-scale co-training [6], [19], [11], [14], [35], [36]. Embodied Chain-of-Thought (ECoT) [19] trains VLAs to generate explicit multi-step reasoning outputs before predicting actions. $\pi_{0.5}$ [6] employs a two-stage strategy that pre-trains on diverse multimodal data to acquire broad semantic priors before fine-tuning a continuous control expert. Recent works further explore reasoning and generalization through π_0 -style co-training or purely autoregressive approaches [11], [14], [35], [37].

c) Embodied Reasoning Benchmarks: To measure embodied reasoning capabilities, the community has developed benchmarks spanning various levels of embodied understanding [38], [39], [40], [41], [42], [43]. Some benchmarks have focused on isolated embodied reasoning facets, such as egocentric perception [44], [41], long-horizon planning [38], [39], or affordance-aware placement [45], [46]. More recently, the community has moved toward comprehensive and systemic evaluation frameworks for embodied reasoning [7], [34], [35]. For instance, ERQA[7] pioneered the integration of capabilities essential for physical world interaction—including spatial awareness, trajectory reasoning, and task-level awareness—to synthesize abstract reasoning with concrete actions. Similarly, ShareRobot-Bench[34] and MMRo[40] establish multi-dimensional scaffolds to quantify high-level cognition and system-level robustness. Addressing the limitations of benchmarks that focus solely on execution success, RoboBench[47] introduces a holistic evaluation of the manipulation pipeline, spanning perception, reasoning, generalized planning, affordance prediction, and failure analysis.

B. Vision-Language-Action Models

Current VLA architectures predominantly fall into two categories based on their action representation strategies.

a) Discrete Quantization and Autoregressive Tokenization: A prominent class of VLAs transforms continuous robotic actions into discrete tokens, allowing the model to treat action prediction as a next-token

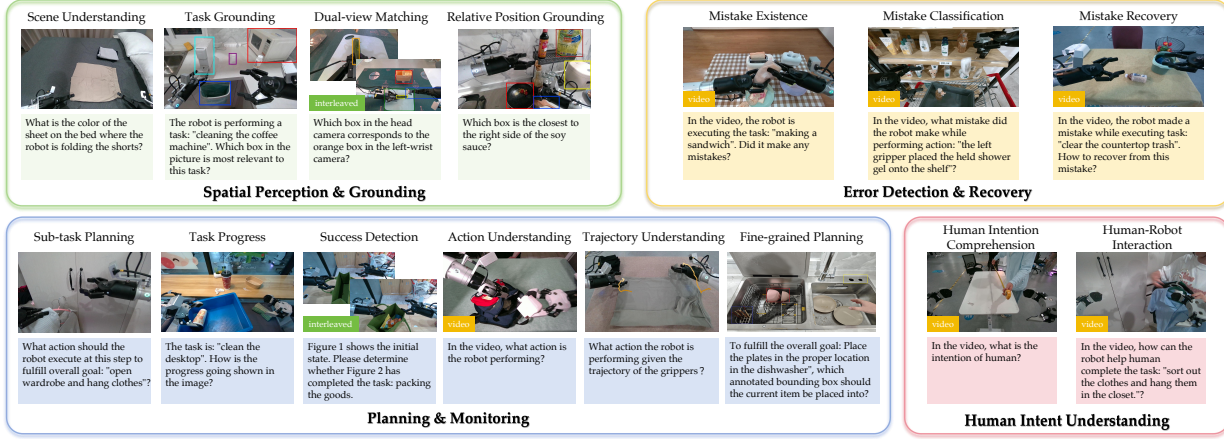


Fig. 2: Illustration of the ERIQ benchmark. Example samples from the four major categories of embodied reasoning.

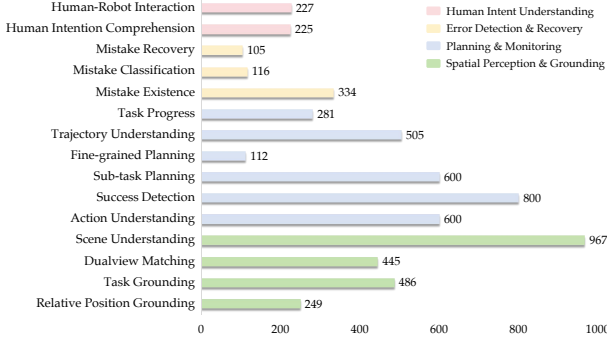


Fig. 3: Distribution of the ERIQ benchmark across its 15 fine-grained sub-tasks.

prediction task similar to natural language [2], [3], [19], [21], [48], [16], [49]. While this approach benefits from the mature optimization landscape of Transformer-based VLMs, it is constrained by the precision-efficiency trade-off. Concretely, simple uniform binning requires an excessively large vocabulary to achieve the resolution necessary for fine motor control [3], whereas learned quantization methods suffer from imprecise execution [21]. Recent attempts like FAST [12] utilize byte-pair encoding (BPE) to achieve compact action compression, which introduce variable-length sequence structures that destabilize autoregressive decoding.

b) Continuous Control via Generative Action Heads: To achieve the high-fidelity control required for dexterous tasks, several recent works have integrated continuous action representations using diffusion or flow-matching objectives [50], [4], [5], [51], [6], [17], [52], [13], [35], [37], [16]. While these generative heads offer superior precision, they often face significant optimization conflicts when paired with discrete VLM backbones. Specifically, high-frequency gradients from the action-denoising objective can interfere with

and degrade the VLM’s pre-trained semantic reasoning capabilities. Current literature addresses this through complex architectural safeguards: Driess et al. [20] propose “Knowledge Insulation” to block gradient flow into the backbone, while ChatVLA [14] utilizes “Phased Alignment” to incrementally synchronize multimodal modalities.

III. EMBODIED REASONING AND ERIQ BENCHMARK

To achieve broad generalization in robotic manipulation, a robot must possess robust “embodied reasoning”, the capacity to synthesize spatial awareness, temporal dynamics, and causal logic to plan and correct actions. However, evaluating this capability within end-to-end VLA models is challenging; when a robot fails a task, it is often unclear whether the failure stems from a lack of high-level semantic understanding or low-level motor execution errors. To address this ambiguity, we argue for decoupling the evaluation of reasoning from physical execution. Therefore, we introduce a benchmark designed to evaluate the VLM’s embodied reasoning capabilities independently of motor execution.

A. Embodied Reasoning Intelligence Quotient (ERIQ) Benchmark

We introduce ERIQ, a large-scale benchmark containing 6,052 embodied question-answering pairs. ERIQ employs a standardized Visual Question Answering (VQA) protocol to quantify embodied comprehension independently of control policies.

The ERIQ benchmark is structured as a multi-dimensional framework assessing four pillars of embodied reasoning: (1) Spatial Perception & Grounding, (2) Planning & Monitoring, (3) Error Detection & Recovery, and (4) Human Intent Understanding. Collectively, these domains comprise 15 carefully designed sub-tasks

TABLE I: Comparison of ERIQ with other embodied reasoning benchmarks. Data is strictly aligned with the source: ERIQ (Ours) achieves full support (●) across all reasoning dimensions and physical data attributes compared to existing benchmarks. Reg. denotes regression metrics for continuous values.

Benchmark	Type	Test Scale (QA Pairs)	Data Source		Reasoning Dimensions			Evaluation Method
			Robo View	Real-world Data	Spatial	Plan	Error	
RoboSpatial-home [43]	Image	350	○	●	●	○	○	○
RoboSpatial-val [43]	Image	6,000	○	●	●	○	○	○
EmbodiedBench [42]	Image	1128	●	○	●	●	●	○
EmbodiedEval [53]	Image	328	○	○	●	●	○	○
EgoThink [41]	Image	700	○	●	●	●	○	○
EO-bench [35]	Image	648	●	●	●	●	○	○
MMRo [40]	Image	26,175	●	●	●	●	○	○
								MC/LLM+Human based Open-ended/Reg.
Cosmos-Reason1 [54]	Video	1,205	●	●	●	●	●	○
EgoPlan [39]	Video	1,584	○		○	●	○	○
ERQA [7]	Video	400	●	●	●	●	○	○
RoboVQA [38]	Video	1,000	●	●	○	●	●	○
OpenEQA [44]	Video	2,193	○	●	●	●	○	○
VidEgoThink [55]	Video	4,993	○	●	●	●	●	○
ShareRobot-Bench [34]	Video	3,442	●	●	●	●	○	○
RoboBench [47]	Video	6,092	●	●	●	●	●	●
ERIQ (Ours)	Video	6,052	●	●	●	●	●	MC

●: Fully Supported ○: Partially Supported ○: Not Supported

that measure perception, reasoning, error handling, and human intent understanding in real-world physical contexts. Each sub-task adheres to a standardized multiple-choice or binary (Yes/No) format, enabling deterministic, straightforward evaluation. This design eliminates the ambiguity of open-ended generation metrics, ensuring fairness and reproducibility. A visual overview of the ERIQ benchmark QA samples is shown in Figure 2.

a) Spatial Perception and Grounding: A prerequisite for deliberate robotic action is the ability to perceive and interpret the environment. This domain tests global and relational understanding through tasks such as *Scene Understanding*, *Task Grounding*, and *Relative Position Grounding*. These tasks assess an agent’s ability to resolve object referents from complex instructions (e.g., “the bowl to the left of the cutting board”) and to solve the symbol grounding problem in cluttered scenes.

b) Task Planning and Execution Monitoring: Intelligent agents must reason over causal structures to achieve complex goals. This domain includes *Sub-task Planning* and *Trajectory Analysis*, evaluating whether the agent can decompose high-level instructions into coherent action sequences and recognize task completion through visual state transitions.

c) Error Detection and Recovery: Robust operation requires diagnosing and recovering from failures. We establish a hierarchy—*Mistake Existence*, *Classification*, and *Recovery*—to measure the agent’s ability to recognize errors (e.g., gripper slip), attribute causes, and propose corrective actions without requiring physical execution.

d) Human Intent Understanding: Effective collaboration requires reasoning about the goals of other agents. We assess this via *Human Intention Compre-*

hension, where the agent must infer human goals from video context to anticipate cooperative actions, treating collaboration as an embodied reasoning task.

The distribution of the ERIQ benchmark across its 15 fine-grained sub-tasks is shown in Figure 3. The dataset is constructed from over 100 distinct task scenarios spanning five domains: household (35%), restaurant (20%), supermarket (20%), industrial (15%), and office (10%). To assess multi-modal reasoning comprehensively, the dataset integrates three modalities: Single Image (53%) for foundational perception, Sequential Images (26%) for temporal dynamics, and Interleaved Image–Text Sequences (21%) for context-rich reasoning.

Despite the expanding scope of existing embodied reasoning benchmarks, they frequently treat task failure as a terminal diagnostic state, overlooking the closed-loop reasoning required for actionable error recovery. Furthermore, dimensions such as human intent inference and collaborative reasoning remain largely absent from current assessments. As illustrated in Table I, ERIQ establishes a new frontier in embodied reasoning by providing a more comprehensive evaluation suite to date. Unlike existing benchmarks that offer fragmented support, ERIQ is the only framework to provide exhaustive, full coverage (●) across all four critical reasoning dimensions: *Spatial Awareness*, *Temporal Planning*, *Error Detection & Recovery*, and *Human Intent Understanding*. In stark contrast, even large-scale benchmarks such as MMRo [40] or specialized ones like EgoPlan [39] focus primarily on fundamental spatial or planning tasks, leaving high-order cognitive dimensions like Error Recovery and Human Intent Understanding either entirely absent or only partially addressed (○). ERIQ comprises 6,052 QA pairs, all of which are derived entirely from

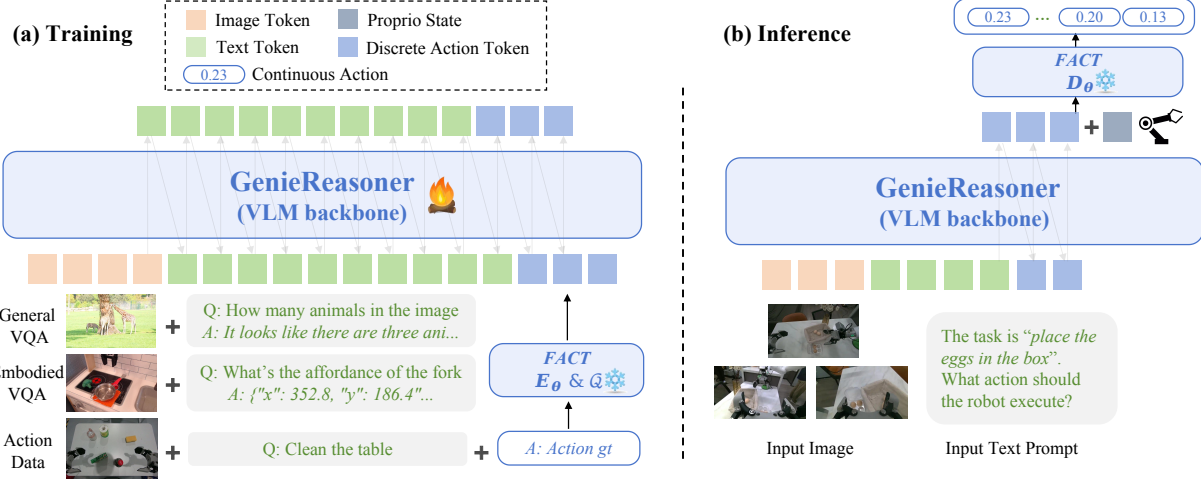


Fig. 4: The GenieReasoner system architecture. (a) Training: Our unified pipeline jointly optimizes the VLM backbone for multimodal reasoning and robotic control by tokenizing continuous actions into a discrete latent space. This process encompasses the second and third stages of the training recipe (Section V-A), where General VQA data is incorporated during the second stage to preserve foundational vision-language knowledge. (b) Inference: Discrete action codes generated by the VLM backbone are decoded into continuous control signals via the FACT decoder, ensuring high-precision manipulation that is semantically grounded in the task instructions.

authentic, real-world robotic trials to ensure a faithful first-person *Robo View* perspective. By adopting a deterministic Multiple Choice (MC) evaluation protocol, ERIQ eliminates the subjectivity and noise inherent in LLM-based scoring or human-based open-ended evaluations, providing a rigorous and reproducible diagnostic tool for advancing robust, general-purpose VLA models.

Leveraging this ERIQ benchmark, our subsequent experiments in Section V demonstrate a clear correlation between strong reasoning scores on ERIQ and superior success rates in end-to-end manipulation tasks, validating that a stronger reasoning backbone is a foundational driver of generalized robotic control.

IV. GENIEREASONER: UNIFIED DISCRETE LOW-LEVEL POLICY FRAMEWORK

A. Preliminaries

We formulate the generalist robotic manipulation task as a learning problem for a policy π_θ , parameterized by θ . The system receives a multimodal observation stream and operates within a continuous action space $\mathcal{A} \subset \mathbb{R}^S$ (e.g., end-effector pose and gripper state). At each time step τ , the observation \mathbf{o}_τ comprises T_{obs} images $\mathbf{I}_\tau \in \mathbb{R}^{T_{obs} \times h \times w \times 3}$ and a natural language instruction l .

Following the Vision-Language-Action (VLA) route, we cast policy learning as a multimodal action generation task. Specifically, the objective is to maximize the log-likelihood of predicting future action chunks $\mathbf{a}_{\tau:\tau+H} \in \mathbb{R}^{H \times S}$ conditioned on the current observation and instruction, where H denotes the prediction horizon.

The optimization objective over a demonstration dataset \mathcal{D} is formulated as:

$$\theta^* = \operatorname{argmax}_\theta \mathbb{E}_{\zeta \sim \mathcal{D}} \left[\sum_{\tau=1}^{|\zeta|} \log p_\theta(\mathbf{a}_{\tau:\tau+H} \mid \mathbf{I}_\tau, l) \right], \quad (1)$$

where $|\zeta|$ denotes the episode length. The model π_θ serves as a unified conditional probability estimator mapping high-dimensional multimodal inputs to precise low-level control signals.

B. System Architecture

To effectively ground the semantic reasoning of VLMs into high-precision robotic control, we must reconcile the conflict between the model’s discrete autoregressive backbone and the continuous nature of motor execution. Existing discretization strategies face distinct limitations: uniform binning necessitates an excessive number of tokens to match the resolution required for manipulation [3], [2]; learned quantization (e.g., VQ-VAE) achieves compactness but lacks high-precision control [21]; and rule-based adaptive methods (e.g., FAST [12]) introduce decoding instability due to their non-deterministic sequence lengths [23].

To address these issues, we introduce FACT (Flow-matching Action Tokenizer). Our key insight is to combine VQ-VAE-style discretization with a flow-matching decoding head [56]. By shifting the burden of fine-grained motion generation from the discrete latent resolution to a generative decoding process, FACT enables

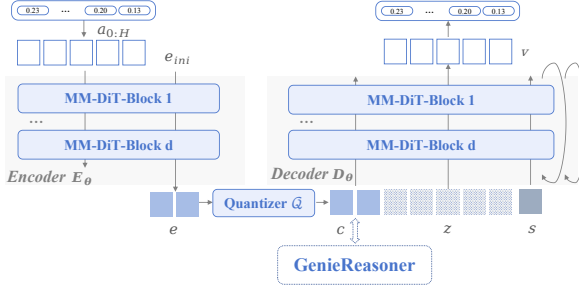


Fig. 5: The FACT Action Tokenizer. We discretize continuous robot actions into compact tokens via a VQ-encoder, enabling autoregressive modeling by the VLM. To preserve control precision, the decoder utilizes flow matching to reconstruct smooth, continuous trajectories from the quantized tokens and Gaussian noise z .

the VLM to plan in a compact, stable discrete space while recovering high-fidelity, continuous trajectories via Ordinary Differential Equation integration.

Based on FACT, we propose the GenieReasoner system, which is illustrated in Figure 4. The system operates in two phases: (1) Training (Figure 4a): We employ a unified pipeline that jointly trains the VLM on multimodal reasoning and robotic control. By tokenizing continuous action sequences into a sequence of discrete action tokens, the VLM backbone learns to map multimodal observations and high-level instructions to compact action tokens. (2) Inference (Figure 4b): During deployment, the discrete action codes generated by the VLM backbone are mapped back to continuous control signals via the FACT decoder. By solving the probability flow ODE, the decoder ensures high-precision manipulation that is semantically grounded in the task instruction. This integrated framework allows GenieReasoner to leverage the reasoning prowess of VLMs while maintaining the dexterity and precision required for complex robotic tasks.

C. FACT: Flow-matching Action Tokenizer

The FACT architecture comprises a VQ-encoder \mathcal{E}_θ and a flow-matching decoder \mathcal{D}_θ . For the backbone of both components, we employ the Multimodal Diffusion Transformer (MM-DiT) architecture [57], configured to process sequences with a patch size of one.

a) Encoder and Quantization: The tokenization process begins by standardizing the action chunk to yield $\mathbf{a}_{0:H} \in \mathbb{R}^{H \times S}$. The encoder \mathcal{E}_θ maps this input to a continuous latent representation $e \in \mathbb{R}^{L \times D}$, performing both temporal ($L \leq H$) and spatial ($D \leq S$) compression. As shown in Figure 5, we use zero-initialized queries e_{ini} to interact with action features:

$$e = \mathcal{E}_\theta(\mathbf{a}_{0:H}, e_{ini}). \quad (2)$$

To obtain a discrete representation, we employ a bitwise quantizer following the lookup-free quantization method [58]. The continuous embedding e is mapped to a discrete code $c \in \{-1, +1\}^{L \times D}$ based on the sign of its elements:

$$c = \mathcal{Q}(e) = \text{sign}(e). \quad (3)$$

b) Flow-Matching Decoder: We train the decoder network \mathcal{D}_θ using the Rectified Flow objective [56]. The goal is to learn the velocity field along a straight-line trajectory that transports samples from a standard Gaussian distribution to the data distribution. This trajectory is defined by the linear interpolation:

$$a^{(t)} = (1 - t)z + ta, \quad t \in [0, 1], \quad (4)$$

where $z \sim \mathcal{N}(0, I)$ is the noise sample and a is the target action chunk. The target constant velocity along this path is simply $v^{(t)} = \frac{d}{dt}a^{(t)} = a - z$. The decoder is trained to predict this velocity $v^{(t)}$ given the noisy state $a^{(t)}$, the flow time step t , and the condition c :

$$v^{(t)} = \mathcal{D}_\theta(a^{(t)}, c, t). \quad (5)$$

Note the condition c is the quantized latent code from the encoder in our context. Architecturally, t is injected into the MM-DiT blocks via AdaLN modulation, allowing the model to adapt its predictions across the integration trajectory.

c) Training Loss: The training objective combines quantization regularization with the flow-matching loss. Following [58], we apply entropy and commitment losses to the quantization process. The entropy loss maximizes codebook usage over the empirical distribution of codes within a batch, denoted as $\bar{p}(c)$:

$$\mathcal{L}_{\text{entropy}} = \mathbb{E}_{a \sim \mathcal{D}} [H(\bar{p}(c | a))] - H(\bar{p}(c)). \quad (6)$$

The commitment loss ensures the continuous embedding stays close to its quantized value:

$$\mathcal{L}_{\text{commit}} = \mathbb{E}_{a \sim \mathcal{D}} \left[\|e - \bar{p}(c)\|_2^2 \right]. \quad (7)$$

The flow-matching loss for the decoder network \mathcal{D}_θ is formulated as a simple mean-squared error objective:

$$\mathcal{L}_{\text{flow}} = \mathbb{E}_{a, z, t \sim \mathcal{U}[0, 1]} \left[\left\| (a - z) - \mathcal{D}_\theta(a^{(t)}, c, t) \right\|_2^2 \right]. \quad (8)$$

d) Inference and Integration: At inference time, the VLA policy π_θ autoregressively predicts the sequence of discrete action codes \hat{c} . These codes are passed to the pre-trained decoder \mathcal{D}_θ to generate the continuous action trajectory. Technically, we solve the Ordinary Differential Equation (ODE) defined by the learned velocity field, utilizing a flow integration time variable $t \in [0, 1]$ to distinguish the generative process

from the physical action timesteps. Specifically, starting from Gaussian noise $\hat{a}^{(t=0)} \sim \mathcal{N}(0, I)$ at $t = 0$, we numerically integrate the velocity predicted by the decoder, where the decoder takes the current intermediate state \hat{a}^t (rather than just the initial noise) as input:

$$\hat{a}^{(t+\Delta t)} = \hat{a}^{(t)} + \Delta t \cdot \mathcal{D}_\theta(\hat{a}^{(t)}, \hat{c}, t), \quad (9)$$

$$\hat{a} = \hat{a}^{(t=0)} + \int_0^1 \mathcal{D}_\theta(\hat{a}^{(t)}, \hat{c}, t) dt. \quad (10)$$

The reconstructed action $\hat{a} = \hat{a}^{(t=1)}$ is subsequently executed by the robot controller. This inference procedure bridges high-level reasoning and low-level motor control: the policy generates discrete and semantically grounded action tokens, while the diffusion decoder ensures high-fidelity and physically feasible motion reconstruction.

V. EXPERIMENTS

We evaluate the GenieReasoner framework through a systematic analysis of its embodied reasoning capability, tokenizer architecture, and training strategy. We investigate four core research questions. First, can *embodied reasoning* be measured independently of action control, and does this metric reliably predict downstream manipulation success? Second, can FACT accurately reconstruct precise actions from compact discrete tokens? Third, what is the impact of introducing embodied data at different stages of the training pipeline (pre-training versus post-training) on final performance? Fourth, does our approach exhibit stronger generalization in real-world tasks compared to continuous (e.g., $\pi_{0.5}$) and discrete (e.g., π_0 -FAST) baselines?

To address these questions, we conduct a comprehensive evaluation that spans multiple components. We first assess embodied reasoning using the ERIQ Benchmark and analyze its correlation with task success. We then measure the reconstruction error and compression efficiency of FACT. Next, we perform end-to-end simulated ablation studies to compare different data mixtures. Finally, we validate real-world performance on different robotic platforms.

A. Implementation Details

a) Training Data: To preserve general visual-language capability while enhancing embodied understanding and reasoning, we curated a mixed-source training dataset that combines generic multimodal data with embodied reasoning-specific datasets. For generic VLM training, we use open-source multimodal datasets including *Cambrian-10M* [59], *LLaVA-OneVision* [60], *Describe Anything* [61], *CogVLM-SFT-311K* [62], and *BLIP3-Grounding-50M* [63], cover-

ing images, videos, dialogue-style QA, and detection-template QA. Parts of these corpora are converted and translated to support bilingual (Chinese/English) training. To strengthen embodied understanding, we further incorporate several open-source embodied-intelligence datasets, such as *NVIDIA Cosmos-Reason* [54], *ShareRobot* [34], *Robo2VLM* [64], *EmbSpatial-SFT* [65], and *ManipulationVQA-60K* [64], which span planning, trajectory reasoning, spatial understanding, and embodied VQA. While publicly available datasets provide broad embodied knowledge, they often exhibit a distributional mismatch with the specific egocentric perspectives required for real-world deployment. To ensure homologous alignment between reasoning and the robot’s observation space, we curated an embodied reasoning dataset based on *AgiBot World* [5], which includes (i) 2D trajectory data, where action sequences are projected onto images from three views (top-head and dual wrists); (ii) grounding annotations combining human labels with automated labels for key-object recognition and localization; (iii) sub-task planning data, which are fully annotated and linguistically rewritten to ensure diversity; and (iv) scene understanding, alongside other essential auxiliary tasks.

For action pre-training, we utilize large-scale embodied demonstrations from the *AgiBot World* platform, multi-embodiment data collected on ARX and AgileX robots, and various open-source manipulation datasets, providing substantial diversity across embodiments, scenes, and actuation styles.

b) Training recipe: We implement a three-stage training strategy comprising two pre-training stages followed by a final post-training stage. In the first stage, we train the FACT tokenizer as in Figure 5 with the loss function described in Section IV-C. In the second stage, we perform end-to-end joint training on a mixture of general VQA data, embodied VQA data, and tokenized action data. This joint pre-training enables the model to simultaneously acquire spatio-temporal grounding and motor control capabilities within a unified representation space. In the third and final stage, we conduct task-specific post-training while maintaining the co-training objective—mixing embodied VQA and action data—to stabilize alignment and prevent the catastrophic forgetting of reasoning capabilities.

B. Embodied Reasoning Capabilities

We first evaluate the embodied reasoning capability of the VLM backbone independently from action execution. This subsection presents qualitative visualizations of spatial and causal reasoning across different robots, followed by quantitative results on our ERIQ Benchmark and open-source datasets. We aim to verify if our pre-training improves embodied understanding while pre-

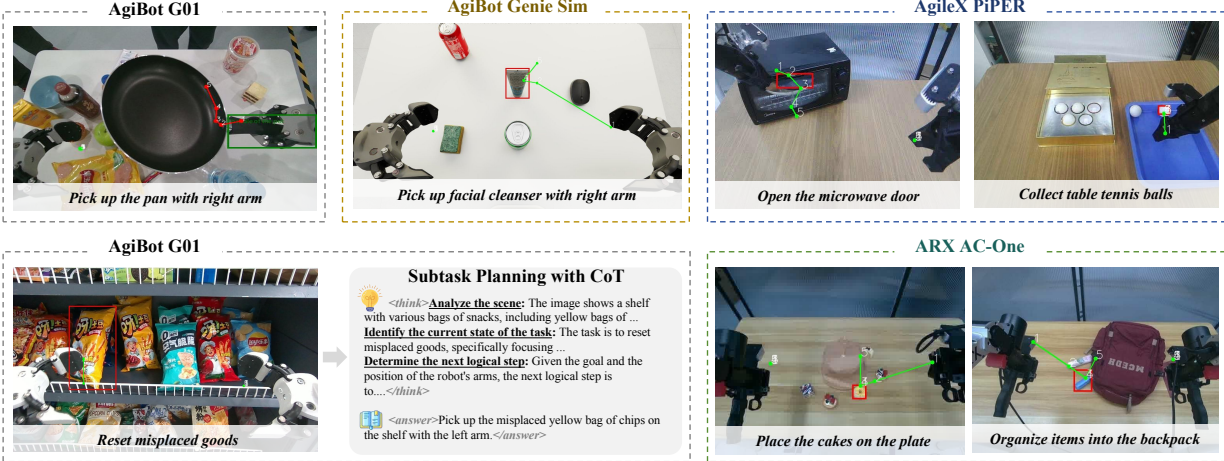


Fig. 6: Qualitative visualization of the VLM’s multi-task reasoning capabilities. We display spatial reasoning, subtask planning, and Chain-of-Thought (CoT) inference across diverse embodiments (AgiBot G01, AgiBot Genie Simulation, AgileX, ARX). These results are generated in a zero-shot setting, demonstrating robust spatial and causal reasoning without task-specific adaptation.

TABLE II: Overall performance evaluation. The table is split into two parts. Part I covers Open-source Spatial Benchmarks and the *Spatial Perception & Grounding* subset of ERIQ Benchmark (including Scene Understanding, Dualview Matching, Task Grounding, and Relative Position Grounding). Part II covers the remaining ER-6K Benchmark subsets: *Planning & Monitoring* (Action Understanding, Success Detection, Subtask Planning, Fine-grained Planning, Trajectory Analysis, and Task Progress), *Human Intent Understanding* (Human Intention Comprehension and Human-Robot Interaction), and *Error Detection & Recovery* (Mistake Existence, Mistake Classification, and Mistake Recovery).

Model	Open-Source Spatial Benchmarks				ERIQ Benchmark			
	CV-Bench	EmbSpa	BLINK-S	BLINK-R	Scene Und.	Dualview	Task Grd.	Rel. Pos.
Qwen2.5-VL-3B	71.29	62.01	81.12	66.94	78.49	37.53	60.08	52.61
Qwen2.5-VL-7B	80.78	70.47	90.21	79.03	86.66	50.56	75.93	73.09
Qwen3-VL-8B	85.69	78.32	86.71	87.10	90.90	81.35	88.27	67.07
InternVL-3.5-8B	82.16	75.11	86.01	79.84	85.94	52.58	81.69	70.28
RoboBrain2.0-7B	86.44	75.80	79.02	83.87	85.73	57.53	78.40	71.08
Cosmos-Reason1-7B	75.20	68.90	84.62	79.84	85.94	53.48	74.69	67.07
Claude-Sonnet-4	75.80	64.29	79.72	72.58	79.83	64.94	66.26	70.28
GPT-4o-mini	85.21	78.29	88.11	79.03	88.00	93.48	90.12	73.90
Gemini-2.5-pro	84.59	78.74	84.62	79.03	88.42	89.89	89.71	70.68
Ours-3B	83.89	70.66	74.83	83.87	84.18	68.54	93.21	77.51

Model	ERIQ Benchmark										ERIQ-Avg	
	Act. Und.	Success	Subtask	Fine-grained	Traj.	Progress	Intention	Interact.	Exist.	Classify		
Qwen2.5-VL-3B	65.50	52.75	55.67	46.43	57.62	25.98	86.22	78.85	34.43	73.28	59.05	58.64
Qwen2.5-VL-7B	76.83	62.62	60.67	54.46	60.40	24.20	73.78	77.53	50.30	72.41	64.76	66.69
Qwen3-VL-8B	89.17	69.38	66.33	65.18	63.76	33.45	89.78	76.65	52.99	86.21	80.00	75.53
InternVL-3.5-8B	78.33	55.00	59.50	59.82	58.42	27.40	80.89	83.26	50.60	74.14	65.71	66.72
RoboBrain2.0-7B	82.33	56.88	61.00	51.79	58.22	24.56	84.89	83.26	50.90	76.72	57.14	67.38
Cosmos-Reason1-7B	86.33	54.75	65.00	53.57	63.37	22.78	84.00	81.94	58.08	69.83	72.38	67.99
Claude-Sonnet-4	67.67	61.50	61.33	62.50	55.84	32.03	92.89	83.26	37.13	84.48	83.81	65.66
GPT-4o-mini	84.67	71.63	65.17	71.43	68.91	49.82	89.78	79.74	66.77	77.59	68.57	77.61
Gemini-2.5-pro	89.83	67.37	76.67	81.25	75.05	62.28	91.11	87.67	67.07	90.52	87.62	80.55
Ours-3B	96.67	85.25	90.50	55.36	73.86	51.60	96.44	83.26	75.45	93.10	85.71	82.72

serving general visual-language capabilities.

1) *Quantitative Comparison on ERIQ Benchmark and Open-source VLM Benchmarks:* We evaluate our embodied VLM on both standard open-source VLM benchmarks and our proposed ERIQ suite to quantify

its general-purpose reasoning and embodied comprehension, as detailed in Section V. On the open-source benchmarks, our model consistently outperforms the base model (Qwen2.5-VL-3B), despite not being explicitly trained on these datasets. This demonstrates that the

TABLE III: **Ablation study on training recipes.** We evaluate the impact of Action Alignment and Embodied VQA (Emb. VQA) across different training stages. To isolate performance bottlenecks, we report (i) ERIQ scores to measure reasoning capabilities immediately following pre-training, (ii) Language Following to assess semantic grounding (reaching the target vicinity), and (iii) Success Rate for end-to-end task completion. Gen. VQA and Emb. VQA denote general and embodied Vision Question Answering datasets. Target, Spatial, and Color represent instruction categories based on direct reference, absolute pose, and visual attributes, respectively.

Exp#	Pre-train			ERIQ ↑	Post-train		Language Following ↑			Success Rate ↑			
	Gen. VQA	Emb. VQA	Action		Emb. VQA	Action	Target	Spatial	Color	Target	Spatial	Color	
#0				58.64			✓	0.24	0.05	0.17	0.05	0.00	0.06
#1	✓	✓		82.72			✓	0.28	0.15	0.25	0.04	0.00	0.03
#2			✓	0.00			✓	0.57	0.45	0.52	0.12	0.20	0.07
#3	✓	✓	✓	80.39			✓	0.78	0.68	0.73	0.18	0.05	0.14
#4	✓	✓	✓	80.39		✓	✓	0.79	0.54	0.91	0.25	0.35	0.22

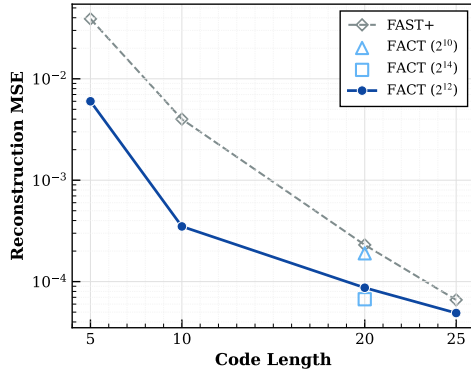


Fig. 7: Reconstruction fidelity analysis. We compare the reconstruction Mean Squared Error (MSE) of our FACT tokenizer against the FAST+ baseline across varying code lengths. FACT achieves lower error rates at equivalent code lengths (e.g., at length 20).

embodied pre-training pipeline preserves—and in many cases enhances—foundational visual–language knowledge, effectively avoiding the capability degradation often associated with domain-specific fine-tuning. On the ERIQ Benchmark, our model demonstrates a significant performance leap, improving the average reasoning score from 58.64% (base) to 82.72%. This confirms the effectiveness of co-training on diverse embodied reasoning specific data in this paper. A fine-grained analysis reveals particularly high proficiency in high-level semantic tasks, such as Action Understanding (96.67%) and Human Intention Comprehension (96.44%). Notably, we observe a substantial gain in Dualview Matching (an absolute increase of 31.01% over the base model) and Relative Position Grounding (+24.9%), indicating that co-training on embodied data specifically strengthens the model’s multi-perspective spatial awareness.

2) *Qualitative results of Generalized Embodied Reasoning:* As shown in Figure 6, we qualitatively demonstrate the model’s robust generalization and spatial rea-

soning capabilities across diverse robotic platforms. We visualize three core outputs: task-oriented grounding, trajectory prediction, and chain-of-thought (CoT) inference, across a variety of tasks and scenes. These include real-world deployments on AgiBot G01, AgileX and ARX platforms, and a high-fidelity simulation environment AgiBot GenieSim[66].

The results reported herein were obtained in a *zero-shot* manner, necessitating no task-specific adaptation. This underscores the robust inherent generalization of our VLM across both spatial and causal reasoning dimensions. These findings validate the framework’s efficacy in facilitating cross-embodiment transfer and operational robustness within unstructured real-world environments.

C. Ablation on FACT Tokenizer

Next, we analyze the performance of the FACT at the representation level. We compare its reconstruction error against the FAST+ baseline [12] across different code lengths and vocabulary sizes in Figure 7. These experiments aim to demonstrate that our flow-matching decoder achieves high-precision control even with compact discrete tokens. To ensure robust evaluation, we conduct the data split at the task level with a ratio of 40 : 1. The results show that FACT achieves substantially lower reconstruction error at the same compressed code length, often outperforming FAST+ by an entire order of magnitude. This confirms that the flow-matching decoder provides a more expressive and stable mapping from discrete tokens back to continuous actions, enabling more compact and accurate action representations. We further perform an ablation over vocabulary size and code length. With a code length of 20, this setting offers an optimal balance between reconstruction fidelity and prediction difficulty, while still outperforming FAST+ by a wide margin. Based on these results, we adopt a 2^{12} -entry vocabulary together with a code length of 20 as the default tokenizer configuration.

D. Ablation of different training recipes

We investigate the impact of incorporating Embodied VQA and Action Alignment at different training stages on the final policy. Using the GenieSim simulator, we compare various data mixtures to identify the optimal recipe for maximizing instruction following and task success. The task requires the robot to identify and pick up a specified target object with a specific arm in a tabletop environment cluttered with diverse distractors. To ensure a rigorous comparison, all model variants are post-trained on a separate dataset comprising 1200 episodes of real-world robotic data. Evaluations were conducted across 50 rollouts per setting across three categories: (1) Target (direct reference), (2) Color (visual attributes), and (3) Spatial (absolute pose). We decouple the evaluation into language following (semantic grounding) and task success (execution), positing that the former is a necessary but insufficient condition for the latter.

a) Embodied VQA as a Foundation for Grounding: Exp #0 serves as a baseline, utilizing the vanilla Qwen2.5-VL-3B model with only general multimodal pre-training. As illustrated in Table III, the comparison between Exp #0 and Exp #1 highlights the critical role of Embodied VQA pre-training. While both variants yield negligible success rates ($< 5\%$) due to a lack of pre-training action alignment, Exp #1 achieves a significantly higher ERIQ score (82.72 vs. 58.64) and improved language-following metrics. This indicates that while Embodied VQA data alone is insufficient for motor execution, it is foundational for establishing the spatial and semantic grounding required for instruction adherence. Having established VQA’s contribution to semantic grounding, we next examine whether Action Alignment enables physical execution.

b) Action Alignment and the ERIQ Advantage:

Introducing Action Alignment in Exp #2 and Exp #3 triggers a substantial performance leap in execution success. For instance, Exp #2 achieves 20% success on absolute pose instructions compared to 0% in Exp #0. This confirms that aligning the discrete token space with continuous actions is a strict prerequisite for end-to-end execution. However, these findings expose a significant methodological bottleneck: evaluating embodied reasoning via end-to-end success rates is resource-intensive, as it mandates the high computational overhead of action training. Our ERIQ Benchmark addresses this by decoupling reasoning from control, enabling efficient evaluation without action alignment while serving as a strong predictor of potential end-to-end success, as evidenced by the high ERIQ score in Exp #1 foreshadowing the performance realized in Exp #4.

c) Optimal Synthesis and Post-training: Finally, Exp #4 achieves the highest overall performance, signif-

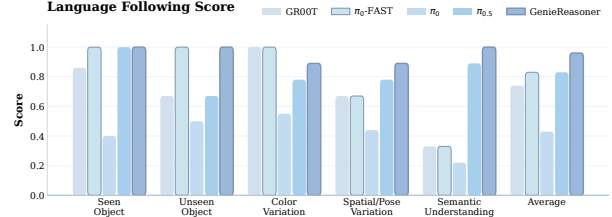


Fig. 8: Real-robot language following evaluation. GenieReasoner consistently outperforms continuous baselines (e.g., π_0 , $\pi_{0.5}$), confirming that aligning the action space with the VLM’s discrete reasoning space significantly reduces target identification errors.

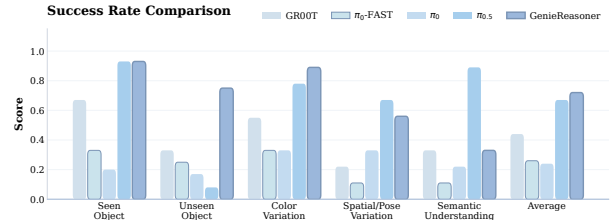


Fig. 9: Real-robot task success rates. This metric measures the full completion of the task, specifically whether the robot successfully grasps and manipulates the target object.

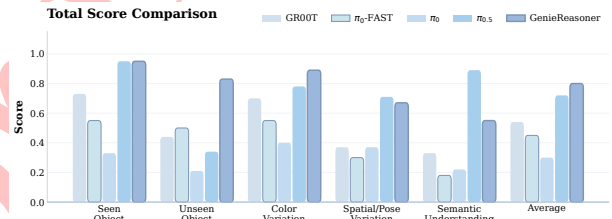


Fig. 10: Overall performance comparison in the real world. This metric prioritizes stable execution while accounting for semantic correctness.

icantly outperforming Exp #3 in success rates (e.g., 0.25 vs. 0.18 on Target) and Color instruction following (0.91 vs. 0.73). The key distinction lies in the post-training recipe: while Exp #3 adopts an “Action Only” approach, Exp #4 retains Embodied VQA data, mirroring the pre-training distribution. This joint post-training preserves the VLM’s reasoning capabilities while simultaneously aligning them with precise action generation, ensuring that high-level planning effectively guides low-level physical execution.

E. Real-World Evaluation

Finally, we assess the operational efficacy of the GenieReasoner system through a series of real-world deployments on AgiBot and ARX robotic platforms. We benchmark our approach against state-of-the-art continuous and discrete baselines across diverse scenarios, specifically focusing on the model’s capacity to han-

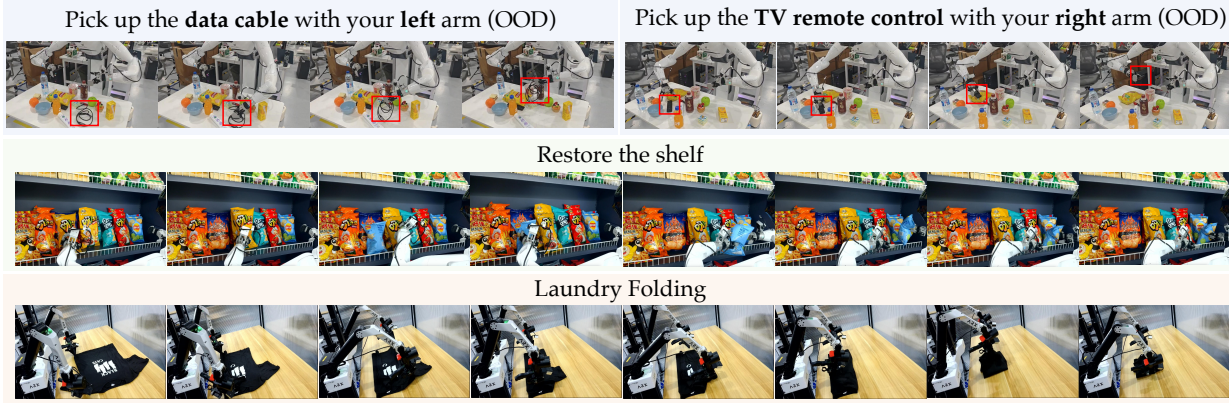


Fig. 11: Visualization of different manipulation tasks in real world.

dle novel object configurations and out-of-distribution instructions. These experiments validate the superior generalization of our unified architecture in unstructured, dynamic environments compared to existing VLA methods.

1) Quantitative Benchmarking on Open-Set Tasks: We conducted real-world robotic experiments to evaluate GenieReasoner against continuous-action baselines (π_0 , $\pi_{0.5}$, GR00T) and a discrete-action baseline (π_0 -FAST) on AgiBot G1. Performance was assessed across five distinct settings of increasing complexity: (1) Seen Object, utilizing objects identical to the training distribution; (2) Unseen Object, introducing novel items not encountered during training; (3) Color Variation, testing robustness to visual shifts in familiar object classes; (4) Spatial/Pose Variation, featuring challenging orientations and extreme placements; and (5) Semantic Understanding, requiring the model to map abstract instructions (e.g., “pick up something to clean the table”) to specific objects. Quantitative results across these dimensions are reported in Figures 8 to 10.

A significant performance gap exists between traditional action representations. The discrete-action baseline, π_0 -FAST, demonstrates superior instruction adherence (high Language Following Score in Figure 8) by effectively leveraging the VLM’s semantic reasoning to identify targets. However, this proficiency does not translate to successful task completion. As shown in Figure 9, its success rate drops precipitously due to quantization artifacts. It cannot represent the continuous precision required for millimeter-level grasping, causing critical alignment failures during physical contact.

Conversely, continuous-action baselines like $\pi_{0.5}$ and GR00T exhibit robust manipulation skills once a target is correctly identified, yet they are highly prone to semantic errors. These models frequently approach the wrong object in complex scenarios, such as the Unseen Object and Color settings (Figure 8). This occurs because their action heads lack direct access to the rich VLM

representations needed for complex reasoning, leading to a weak connection between perception and control.

GenieReasoner effectively resolves this trade-off. By aligning the action space with the VLM’s discrete reasoning while utilizing a flow-matching decoder for high-fidelity reconstruction, our method achieves a synergy that previous architectures lack. It matches the high success rates of continuous policies across all scenarios (Figure 9) while maintaining, and often surpassing, the instruction-following accuracy of discrete models (Figure 8). As summarized in Figure 10, GenieReasoner achieves the highest aggregate score, where the total score is computed as a weighted aggregate: Score = $(1.0 \times \text{Success Rate} + 0.5 \times \text{Following Score})/1.5$, confirming that our factorized action representation enables VLM reasoning to guide precise motor control through flow-matching decoding.

2) Qualitative Analysis of Complex Deployments: To evaluate the cross-embodiment robustness and operational generalization of GenieReasoner, we conducted extensive real-world experiments leveraging both the AgiBot G1 humanoid platform and the ARX AC-One robotic arm. The evaluation protocol consists of three core task categories designed to investigate the integration of high-level semantic grounding with fine-grained motor control: (i) *fine-grained OOD manipulation*, involving the retrieval of out-of-distribution objects (e.g., data cables, TV remotes) in high-entropy, cluttered environments; (ii) *long-horizon semantic tasks*, such as structured shelf restoration; and (iii) *deformable object manipulation*, exemplified by garment folding conducted on the ARX platform. These diverse scenarios require the model to translate abstract multimodal instructions into adaptive, high-precision physical trajectories. Qualitative visualizations of these results across the two distinct robotic embodiments and complex environments are provided in Figure 11.

VI. CONCLUSION

In this work, we demonstrated the necessity of evaluating VLMs independently from action policies and introduced the Embodied Reasoning Intelligence Quotient (ERIQ), a large-scale benchmark designed to systematically diagnose embodied reasoning capabilities across four critical dimensions. To bridge the gap between semantic reasoning and physical execution, we proposed GenieReasoner, a unified VLA architecture powered by the Flow-matching Action Tokenizer (FACT). By converting continuous control into a high-fidelity discrete representation, this design resolves the reasoning-precision trade-off, enabling the consistent co-optimization of high-level planning and low-level action within a single autoregressive framework. Looking forward, we plan to explore deeper synergies between Chain-of-Thought reasoning and action generation, as well as further enhance the system’s generalization and instruction-following robustness across diverse real-world environments.

VII. ACKNOWLEDGMENTS

We gratefully thank Sixian Li and Wenhao Li for their work on benchmark preparation; Da Huang, Junhui Wu, and Qian Wang for simulation support with GenieSim; and Guangte Xiang, Chi Zhang, Yuehan Niu, Ruofei Niu, Jingyuan Wang, Rui Wu, Jia Zeng, and Jingshun Huang for their essential roles in data collection and engineering, hardware deployment, and project promotion.

REFERENCES

- [1] A. Brohan, N. Brown, J. Carbalajal, Y. Chebotar, J. Dabis, C. Finn, K. Gopalakrishnan, K. Hausman, A. Herzog, J. Hsu *et al.*, “Rt-1: Robotics transformer for real-world control at scale,” *arXiv preprint arXiv:2212.06817*, 2022.
- [2] B. Zitkovich, T. Yu, S. Xu, P. Xu, T. Xiao, F. Xia, J. Wu, P. Wohlhart, S. Welker, A. Wahid *et al.*, “Rt-2: Vision-language-action models transfer web knowledge to robotic control,” in *Conference on Robot Learning*. PMLR, 2023, pp. 2165–2183.
- [3] M. J. Kim, K. Pertsch, S. Karamcheti, T. Xiao, A. Balakrishna, S. Nair, R. Rafailov, E. Foster, G. Lam, P. Sanketi *et al.*, “Openvla: An open-source vision-language-action model,” *arXiv preprint arXiv:2406.09246*, 2024.
- [4] K. Black, N. Brown, D. Driess, A. Esmail, M. Equi, C. Finn, N. Fusai, L. Groom, K. Hausman, B. Ichter *et al.*, “ π_0 : A vision-language-action flow model for general robot control. corr, abs/2410.24164, 2024. doi: 10.48550/,” *arXiv preprint ARXIV:2410.24164*.
- [5] Q. Bu, J. Cai, L. Chen, X. Cui, Y. Ding, S. Feng, S. Gao, X. He, X. Hu, X. Huang *et al.*, “Agibot world colosseos: A large-scale manipulation platform for scalable and intelligent embodied systems,” *arXiv preprint arXiv:2503.06669*, 2025.
- [6] K. Black, N. Brown, J. Darpinian, K. Dhabalnia, D. Driess, A. Esmail, M. Equi, C. Finn, N. Fusai *et al.*, “ $\pi_0.5$: a vision-language-action model with open-world generalization,” *arXiv preprint arXiv:2504.16054*, 2025.
- [7] G. R. Team, S. Abeyruwan, J. Ainslie, J.-B. Alayrac, M. G. Arenas, T. Armstrong, A. Balakrishna, R. Baruch, M. Bauza, M. Blokzijl *et al.*, “Gemini robotics: Bringing ai into the physical world,” *arXiv preprint arXiv:2503.20020*, 2025.
- [8] O. M. Team, D. Ghosh, H. Walke, K. Pertsch, K. Black, O. Mees, S. Dasari, J. Hejna, T. Kreiman, C. Xu *et al.*, “Octo: An open-source generalist robot policy,” *arXiv preprint arXiv:2405.12213*, 2024.
- [9] C. Chi, Z. Xu, S. Feng, E. Cousineau, Y. Du, B. Burchfiel, R. Tedrake, and S. Song, “Diffusion policy: Visuomotor policy learning via action diffusion,” *The International Journal of Robotics Research*, vol. 44, no. 10-11, pp. 1684–1704, 2025.
- [10] T. Z. Zhao, V. Kumar, S. Levine, and C. Finn, “Learning fine-grained bimanual manipulation with low-cost hardware,” *arXiv preprint arXiv:2304.13705*, 2023.
- [11] F. Lin, R. Nai, Y. Hu, J. You, J. Zhao, and Y. Gao, “Onetwovla: A unified vision-language-action model with adaptive reasoning,” *arXiv preprint arXiv:2505.11917*, 2025.
- [12] K. Pertsch, K. Stachowicz, B. Ichter, D. Driess, S. Nair, Q. Vuong, O. Mees, C. Finn, and S. Levine, “Fast: Efficient action tokenization for vision-language-action models,” *arXiv preprint arXiv:2501.09747*, 2025.
- [13] Q. Lv, W. Kong, H. Li, J. Zeng, Z. Qiu, D. Qu, H. Song, Q. Chen, X. Deng, and J. Pang, “F1: A vision-language-action model bridging understanding and generation to actions,” *arXiv preprint arXiv:2509.06951*, 2025.
- [14] Z. Zhou, Y. Zhu, M. Zhu, J. Wen, N. Liu, Z. Xu, W. Meng, R. Cheng, Y. Peng, C. Shen *et al.*, “Chatvla: Unified multimodal understanding and robot control with vision-language-action model,” *arXiv preprint arXiv:2502.14420*, 2025.
- [15] D. Qu, H. Song, Q. Chen, Y. Yao, X. Ye, Y. Ding, Z. Wang, J. Gu, B. Zhao, D. Wang *et al.*, “Spatialvla: Exploring spatial representations for visual-language-action model,” *arXiv preprint arXiv:2501.15830*, 2025.
- [16] J. Liu, H. Chen, P. An, Z. Liu, R. Zhang, C. Gu, X. Li, Z. Guo, S. Chen, M. Liu *et al.*, “Hybridvla: Collaborative diffusion and autoregression in a unified vision-language-action model,” *arXiv preprint arXiv:2503.10631*, 2025.
- [17] M. Shukor, D. Aubakirova, F. Capuano, P. Kooijmans, S. Palma, A. Zouitine, M. Aractingi, C. Pascal, M. Russi, A. Marafioti *et al.*, “Smolvla: A vision-language-action model for affordable and efficient robotics,” *arXiv preprint arXiv:2506.01844*, 2025.
- [18] R. Zheng, Y. Liang, S. Huang, J. Gao, H. Daumé III, A. Kolobov, F. Huang, and J. Yang, “Tracevla: Visual trace prompting enhances spatial-temporal awareness for generalist robotic policies,” *arXiv preprint arXiv:2412.10345*, 2024.
- [19] M. Zawalski, W. Chen, K. Pertsch, O. Mees, C. Finn, and S. Levine, “Robotic control via embodied chain-of-thought reasoning,” *arXiv preprint arXiv:2407.08693*, 2024.
- [20] D. Driess, J. T. Springenberg, B. Ichter, L. Yu, A. Li-Bell, K. Pertsch, A. Z. Ren, H. Walke, Q. Vuong, L. X. Shi *et al.*, “Knowledge insulating vision-language-action models: Train fast, run fast, generalize better,” *arXiv preprint arXiv:2505.23705*, 2025.
- [21] Y. Wang, H. Zhu, M. Liu, J. Yang, H.-S. Fang, and T. He, “Vqvla: Improving vision-language-action models via scaling vector-quantized action tokenizers,” *arXiv preprint arXiv:2507.01016*, 2025.
- [22] A. Szot, B. Mazoure, H. Agrawal, R. D. Hjelm, Z. Kira, and A. Toshev, “Grounding multimodal large language models in actions,” *Advances in Neural Information Processing Systems*, vol. 37, pp. 20 198–20 224, 2024.
- [23] X. Luo, X. Yin, H. Wu, L. Gao, and J. Song, “Stable-fast: Stabilizing inference of autoregressive vision-language-action models.”
- [24] M. Ahn, A. Brohan, N. Brown, Y. Chebotar, O. Cortes, B. David, C. Finn, C. Fu, K. Gopalakrishnan, K. Hausman *et al.*, “Do as i can, not as i say: Grounding language in robotic affordances,” *arXiv preprint arXiv:2204.01691*, 2022.
- [25] W. Huang, P. Abbeel, D. Pathak, and I. Mordatch, “Language models as zero-shot planners: Extracting actionable knowledge for embodied agents,” in *International conference on machine learning*. PMLR, 2022, pp. 9118–9147.
- [26] D. Driess, F. Xia, M. S. Sajjadi, C. Lynch, A. Chowdhery,

A. Wahid, J. Tompson, Q. Vuong, T. Yu, W. Huang *et al.*, “Palm-e: An embodied multimodal language model,” 2023.

[27] W. Huang, F. Xia, T. Xiao, H. Chan, J. Liang, P. Florence, A. Zeng, J. Tompson, I. Mordatch, Y. Chebotar *et al.*, “Inner monologue: Embodied reasoning through planning with language models,” *arXiv preprint arXiv:2207.05608*, 2022.

[28] S. Belkhale, T. Ding, T. Xiao, P. Sermanet, Q. Vuong, J. Tompson, Y. Chebotar, D. Dwibedi, and D. Sadigh, “Rt-h: Action hierarchies using language,” *arXiv preprint arXiv:2403.01823*, 2024.

[29] J. Liang, W. Huang, F. Xia, P. Xu, K. Hausman, B. Ichter, P. Florence, and A. Zeng, “Code as policies: Language model programs for embodied control,” *arXiv preprint arXiv:2209.07753*, 2022.

[30] A. Zeng, M. Attarian, B. Ichter, K. Choromanski, A. Wong, S. Welker, F. Tombari, A. Purohit, M. Ryoo, V. Sindhwani *et al.*, “Socratic models: Composing zero-shot multimodal reasoning with language,” *arXiv preprint arXiv:2204.00598*, 2022.

[31] O. Mees, J. Borja-Diaz, and W. Burgard, “Grounding language with visual affordances over unstructured data,” *arXiv preprint arXiv:2210.01911*, 2022.

[32] P. Sharma, A. Torralba, and J. Andreas, “Skill induction and planning with latent language,” in *Proceedings of the 60th Annual Meeting of the Association for Computational Linguistics (Volume 1: Long Papers)*, 2022, pp. 1713–1726.

[33] L. X. Shi, B. Ichter, M. Equi, L. Ke, K. Pertsch, Q. Vuong, J. Tanner, A. Walling, H. Wang, N. Fusai *et al.*, “Hi robot: Open-ended instruction following with hierarchical vision-language-action models,” *arXiv preprint arXiv:2502.19417*, 2025.

[34] Y. Ji, H. Tan, J. Shi, X. Hao, Y. Zhang, H. Zhang, P. Wang, M. Zhao, Y. Mu, P. An *et al.*, “Robobrain: A unified brain model for robotic manipulation from abstract to concrete,” in *Proceedings of the Computer Vision and Pattern Recognition Conference*, 2025, pp. 1724–1734.

[35] D. Qu, H. Song, Q. Chen, Z. Chen, X. Gao, X. Ye, Q. Lv, M. Shi, G. Ren, C. Ruan *et al.*, “Eo-1: Interleaved vision-text-action pretraining for general robot control,” *arXiv preprint arXiv:2508.21112*, 2025.

[36] W. Chen, S. Belkhale, S. Mirchandani, O. Mees, D. Driess, K. Pertsch, and S. Levine, “Training strategies for efficient embodied reasoning,” *arXiv preprint arXiv:2505.08243*, 2025.

[37] S. Yang, H. Li, Y. Chen, B. Wang, Y. Tian, T. Wang, H. Wang, F. Zhao, Y. Liao, and J. Pang, “Instructvla: Vision-language-action instruction tuning from understanding to manipulation,” *arXiv preprint arXiv:2507.17520*, 2025.

[38] P. Sermanet, T. Ding, J. Zhao, F. Xia, D. Dwibedi, K. Gopalakrishnan, C. Chan, G. Dulac-Arnold, S. Maddineni, N. J. Joshi *et al.*, “Robovqa: Multimodal long-horizon reasoning for robotics,” in *2024 IEEE International Conference on Robotics and Automation (ICRA)*. IEEE, 2024, pp. 645–652.

[39] Y. Chen, Y. Ge, Y. Ge, M. Ding, B. Li, R. Wang, R. Xu, Y. Shan, and X. Liu, “Egoplant-bench: Benchmarking multimodal large language models for human-level planning,” *arXiv preprint arXiv:2312.06722*, 2023.

[40] J. Li, Y. Zhu, Z. Xu, J. Gu, M. Zhu, X. Liu, N. Liu, Y. Peng, F. Feng, and J. Tang, “Mmro: Are multimodal llms eligible as the brain for in-home robotics?” *arXiv preprint arXiv:2406.19693*, 2024.

[41] S. Cheng, Z. Guo, J. Wu, K. Fang, P. Li, H. Liu, and Y. Liu, “Egothink: Evaluating first-person perspective thinking capability of vision-language models,” in *Proceedings of the IEEE/CVF Conference on Computer Vision and Pattern Recognition*, 2024, pp. 14 291–14 302.

[42] R. Yang, H. Chen, J. Zhang, M. Zhao, C. Qian, K. Wang, Q. Wang, T. V. Koripella, M. Movahedi, M. Li *et al.*, “Embodiedbench: Comprehensive benchmarking multi-modal large language models for vision-driven embodied agents,” *arXiv preprint arXiv:2502.09560*, 2025.

[43] C. H. Song, V. Blukis, J. Tremblay, S. Tyree, Y. Su, and S. Birchfield, “Robospatial: Teaching spatial understanding to 2d and 3d vision-language models for robotics,” in *Proceedings of the Computer Vision and Pattern Recognition Conference*, 2025, pp. 15 768–15 780.

[44] A. Majumdar, A. Ajay, X. Zhang, P. Putta, S. Yenamandra, M. Henaff, S. Silwal, P. Mcvay, O. Maksymets, S. Arnaud *et al.*, “Openeqa: Embodied question answering in the era of foundation models,” in *Proceedings of the IEEE/CVF conference on computer vision and pattern recognition*, 2024, pp. 16 488–16 498.

[45] W. Yuan, J. Duan, V. Blukis, W. Pumacay, R. Krishna, A. Murali, A. Mousavian, and D. Fox, “Robopoint: A vision-language model for spatial affordance prediction for robotics,” *arXiv preprint arXiv:2406.10721*, 2024.

[46] E. Zhao, V. Raval, H. Zhang, J. Mao, Z. Shangguan, S. Nikolaidis, Y. Wang, and D. Seita, “Manipbench: Benchmarking vision-language models for low-level robot manipulation,” *arXiv preprint arXiv:2505.09698*, 2025.

[47] Y. Luo, C.-K. Fan, M. Dong, J. Shi, M. Zhao, B.-W. Zhang, C. Chi, J. Liu, G. Dai, R. Zhang *et al.*, “Robobench: A comprehensive evaluation benchmark for multimodal large language models as embodied brain,” *arXiv preprint arXiv:2510.17801*, 2025.

[48] Z. Liang, Y. Li, T. Yang, C. Wu, S. Mao, L. Pei, X. Yang, J. Pang, Y. Mu, and P. Luo, “Discrete diffusion vla: Bringing discrete diffusion to action decoding in vision-language-action policies,” *arXiv preprint arXiv:2508.20072*, 2025.

[49] A. Goyal, H. Hadfield, X. Yang, V. Blukis, and F. Ramos, “Vla-0: Building state-of-the-art vlas with zero modification,” *arXiv preprint arXiv:2510.13054*, 2025.

[50] D. G. Octo, H. Walke, K. Pertsch, K. Black, O. Mees, S. Dasari, J. Hejna, C. Xu, J. Luo, T. Kreiman *et al.*, “Octo: An open-source generalist robot policy,” in *Proceedings of Robotics: Science and Systems (RSS)*, 2024.

[51] J. Bjorck, F. Castañeda, N. Cherniadev, X. Da, R. Ding, L. Fan, Y. Fang, D. Fox, F. Hu, S. Huang *et al.*, “Gr0t n1: An open foundation model for generalist humanoid robots,” *arXiv preprint arXiv:2503.14734*, 2025.

[52] H. Shi, B. Xie, Y. Liu, L. Sun, F. Liu, T. Wang, E. Zhou, H. Fan, X. Zhang, and G. Huang, “Memoryvla: Perceptual-cognitive memory in vision-language-action models for robotic manipulation,” *arXiv preprint arXiv:2508.19236*, 2025.

[53] Z. Cheng, Y. Tu, R. Li, S. Dai, J. Hu, S. Hu, J. Li, Y. Shi, T. Yu, W. Chen, L. Shi, and M. Sun, “Embodydeval: Evaluate multimodal llms as embodied agents,” 2025. [Online]. Available: <https://arxiv.org/abs/2501.11858>

[54] A. Azzolini, J. Bai, H. Brandon, J. Cao, P. Chattopadhyay, H. Chen, J. Chu, Y. Cui, J. Diamond, Y. Ding *et al.*, “Cosmosreason1: From physical common sense to embodied reasoning,” *arXiv preprint arXiv:2503.15558*, 2025.

[55] S. Cheng, K. Fang, Y. Yu, S. Zhou, B. Li, Y. Tian, T. Li, L. Han, and Y. Liu, “Videogothink: Assessing egocentric video understanding capabilities for embodied ai,” *arXiv preprint arXiv:2410.11623*, 2024.

[56] X. Liu, C. Gong, and Q. Liu, “Flow straight and fast: Learning to generate and transfer data with rectified flow,” *arXiv preprint arXiv:2209.03003*, 2022.

[57] W. Peebles and S. Xie, “Scalable diffusion models with transformers,” in *Proceedings of the IEEE/CVF international conference on computer vision*, 2023, pp. 4195–4205.

[58] L. Yu, J. Lezama, N. B. Gundavarapu, L. Versari, K. Sohn, D. Minnen, Y. Cheng, V. Birodkar, A. Gupta, X. Gu *et al.*, “Language model beats diffusion–tokenizer is key to visual generation,” *arXiv preprint arXiv:2310.05737*, 2023.

[59] P. Tong, E. Brown, P. Wu, S. Woo, A. J. V. IYER, S. C. Akula, S. Yang, J. Yang, M. Middepogu, Z. Wang *et al.*, “Cambrian-1: A fully open, vision-centric exploration of multimodal llms,” *Advances in Neural Information Processing Systems*, vol. 37, pp. 87 310–87 356, 2024.

[60] B. Li, Y. Zhang, D. Guo, R. Zhang, F. Li, H. Zhang, K. Zhang, P. Zhang, Y. Li, Z. Liu *et al.*, “Llava-onevision: Easy visual task transfer,” *arXiv preprint arXiv:2408.03326*, 2024.

[61] L. Lian, Y. Ding, Y. Ge, S. Liu, H. Mao, B. Li, M. Pavone,

M.-Y. Liu, T. Darrell, A. Yala *et al.*, “Describe anything: Detailed localized image and video captioning,” *arXiv preprint arXiv:2504.16072*, 2025.

[62] W. Wang, Q. Lv, W. Yu, W. Hong, J. Qi, Y. Wang, J. Ji, Z. Yang, L. Zhao, S. XiXuan *et al.*, “Cogvlm: Visual expert for pretrained language models,” *Advances in Neural Information Processing Systems*, vol. 37, pp. 121475–121499, 2024.

[63] L. Xue, M. Shu, A. Awadalla, J. Wang, A. Yan, S. Purushwalkam, H. Zhou, V. Prabhu, Y. Dai, M. S. Ryoo *et al.*, “xgen-mm (blip-3): A family of open large multimodal models,” *arXiv preprint arXiv:2408.08872*, 2024.

[64] K. Chen, S. Xie, Z. Ma, P. R. Sanketi, and K. Goldberg, “Robo2vlm: Visual question answering from large-scale in-the-wild robot manipulation datasets,” *arXiv preprint arXiv:2505.15517*, 2025.

[65] M. Du, B. Wu, Z. Li, X.-J. Huang, and Z. Wei, “Embspatial-bench: Benchmarking spatial understanding for embodied tasks with large vision-language models,” in *Proceedings of the 62nd Annual Meeting of the Association for Computational Linguistics (Volume 2: Short Papers)*, 2024, pp. 346–355.

[66] G. Team, “Geniesim,” 2025. [Online]. Available: https://github.com/AgibotTech/genie_sim

Draft